

Rapid Communications

The Rapid Communications section is intended for the accelerated publication of important new results. Manuscripts submitted to this section are given priority in handling in the editorial office and in production. A Rapid Communication may be no longer than 3½ printed pages and must be accompanied by an abstract. Page proofs are sent to authors, but, because of the rapid publication schedule, publication is not delayed for receipt of corrections unless requested by the author.

Evolution of mass and charge asymmetry in damped heavy-ion reactions

R. T. de Souza, W. U. Schröder, and J. R. Huizenga

*Department of Chemistry and Nuclear Structure Research Laboratory, University of Rochester,
Rochester, New York 14627*

R. Planeta, K. Kwiatkowski, and V. E. Viola

*Department of Chemistry and Indiana University Cyclotron Facility, Indiana University,
Bloomington, Indiana 47405*

H. Breuer

Department of Physics, University of Maryland, College Park, Maryland 20742

(Received 31 December 1987)

Projectile-like fragments have been studied with high A and Z resolution for the damped reactions $^{238}\text{U} + ^{40}\text{Ca}$, ^{48}Ca , ^{58}Ni , and ^{64}Ni at 8.5 MeV/nucleon. These dinuclear systems exhibit widely different driving forces. Qualitative agreement between experiment and dynamical nucleon-exchange transport theory is obtained for the first and second moments of the fragment atomic (Z) and neutron (N) number distributions. However, systematic differences exist between the experimental and theoretical average values of Z and N suggesting the need for more realistic driving forces.

The dependence of mass and charge exchange in heavy-ion collisions on the amount of kinetic energy dissipated into intrinsic degrees of freedom is a subject of great interest.^{1,2} Current reaction theory,^{3,4} successful in explaining a number of damped reaction features, predicts a complex dependence of the fragment A (mass number) and Z (atomic number) distributions on the static potential-energy surface (PES). The present series of high-resolution experiments were designed to study the role of the PES in the nucleon exchange process. In particular, the gradient of the PES is examined in terms of its influence on the driving force affecting the first moments in the proton and neutron number distributions of projectile-like fragments. The second moments, although essential to the description of these distributions, are less sensitive to the PES. The reactions $^{238}\text{U} + ^{40}\text{Ca}$, ^{58}Ni , ^{64}Ni , and ^{48}Ca , at a bombarding energy of 8.5 MeV/nucleon, were chosen for a detailed study of systems with similar mass asymmetry, but very different PES. The N/Z (where N is the neutron number) values of the above projectiles, which reflect directly the gradient in the PES, are very different, namely, 1.00, 1.07, 1.29, and 1.40, respectively. Comparison between experimental results and theoretical predictions have been facilitated by recent advancements in the understanding of the partitioning of excitation energy⁵ between primary fragments. The present experiments were designed to explore a much

wider difference in potential-energy surfaces than earlier such studies of several targets bombarded with ^{56}Fe projectiles.^{6,7}

The experiments were conducted at the Lawrence Berkeley Laboratory's SuperHILAC accelerator where beams of ^{40}Ca , ^{48}Ca , ^{58}Ni , and ^{64}Ni at $E_{\text{lab}}/A = 8.5$ MeV/nucleon bombarded monoisotopic ^{238}U targets of thicknesses ranging from 0.5–1.2 mg/cm². Channel plates, silicon detectors, and ionization chambers were used in the different measurements. Identification of the atomic and mass numbers of the reaction products was performed using a ΔE - E and a time-of-flight (ΔE - E -TOF) technique, respectively. These experimental methods have been described in detail elsewhere.^{7,8} The experimental resolution achieved was 0.4 to 0.7 units full width at half maximum (FWHM) in Z and 0.6 units (FWHM) in A . The simultaneous measurements of A and Z were made at laboratory angles just forward of the corresponding grazing angles. In addition, to ascertain that the data were not biased by the limited center-of-mass angular region spanned by the TOF detector, angular distributions of all elements were measured for each reaction studied.

A representation of the drift in the average proton number $\langle Z \rangle$ of the projectile-like fragment as a function of energy loss is given in Fig. 1 for all four systems. The quantity $(\langle Z \rangle - Z_P)$ represents the difference between the

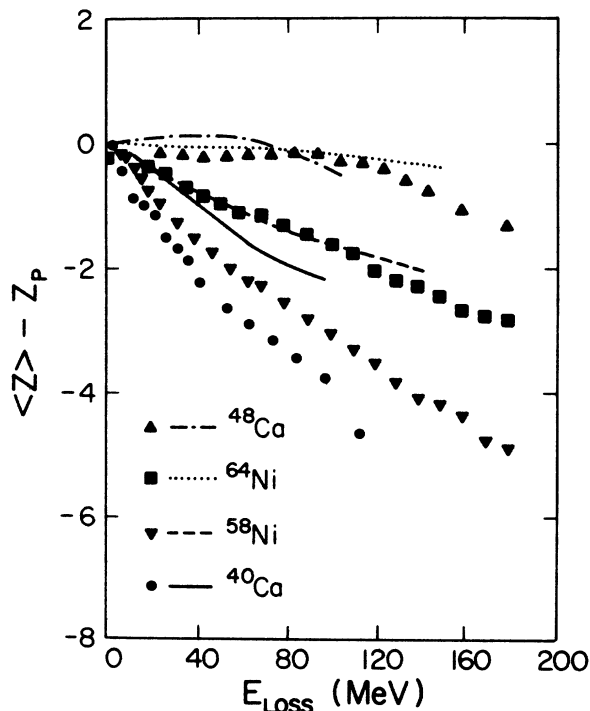


FIG. 1. Proton drift (average measured atomic number minus the atomic number of the projectile) as a function of energy loss for the $^{238}\text{U} + ^{40,48}\text{Ca}$ and $^{238}\text{U} + ^{58,64}\text{Ni}$ reactions at a bombarding energy of 8.5 MeV/nucleon. The experimental data sets (points) and theoretical predictions (lines) are identified in the legend. The predicted primary distributions are corrected for particle evaporation with the statistical evaporation code PACE (Ref. 9). The systematic errors are approximately $\pm 0.3 Z$ units.

measured average charge of the projectile-like fragment and the atomic number of the projectile. Fission events have been eliminated from the data sets. The experimental data reflect the combined effect of two different processes, proton exchange between the two heavy ions during the collision, and subsequent charged-particle evaporation from the excited primary fragments. While the particle evaporation process can only lower the charge of the projectile-like fragment, the nucleon exchange process can, in principle, cause the projectile-like fragment to experience a net proton loss or gain. Calculations with the PACE code⁹ show that the effect of charged-particle evaporation is small, 0.5 unit for the highest energy losses. Hence, the observed decrease of $\langle Z \rangle - Z_P$ with increasing energy loss for the different systems is a direct measure of the primary proton exchange process.

The proton drifts, as observed in Fig. 1, correlate strongly with the projectile N/Z values. Previous results⁷ obtained with ^{56}Fe projectiles agree with these systematics. The magnitudes of the proton drift reflect the gradients in the liquid-drop potential-energy surface (PES) with shell and proximity corrections.¹ This surface is calculated for classical trajectories as a function of angular momentum for all binary fragmentations of the dinuclear system. The four systems discussed here show striking

differences in their potential-energy gradients. For example, the $^{238}\text{U} + ^{40}\text{Ca}$ system has a strong driving force ($\Delta V/\Delta Z = 8$ MeV) to transfer to the target-like fragment (TLF) whereas the $^{238}\text{U} + ^{48}\text{Ca}$ system experiences an insignificant driving force to effect net charge transfer. The $^{58,64}\text{Ni}$ systems represent intermediate cases in the expected order. As seen in Fig. 1, at an E_{loss} of 100 MeV, the $^{238}\text{U} + ^{40}\text{Ca}$ and $^{238}\text{U} + ^{48}\text{Ca}$ systems have transferred on the average 3.6 and zero protons to the TLF, respectively.

Complementary to the $\langle Z \rangle - Z_P$ data, plots of the measured values of $\langle N \rangle - N_P$ are shown in Fig. 2 as functions of E_{loss} for the four reactions studied. Interpretation of these data in terms of neutron exchange must account for the sizable amount of neutron evaporation from the excited primary fragments. Even so, there is an evident difference in the behavior of systems with the neutron-rich projectiles ^{48}Ca and ^{64}Ni and the projectiles ^{40}Ca and ^{58}Ni . In the case of the latter projectiles, for example, the secondary fragments even show a net gain in neutron number. Potential-energy surface calculations indicate that the $^{238}\text{U} + ^{40}\text{Ca}$ system has a strong driving force ($\Delta V/\Delta N = -12$ MeV) for transfer of neutrons to the projectile-like fragment (PLF) whereas the $^{238}\text{U} + ^{48}\text{Ca}$ system has no driving force to effect net neutron transfer. While a direct correlation exists between the experimental proton drift and the N/Z value of the projectile, a similarly systematic behavior is not rigorously observed for the neutron drifts. In Fig. 2, an inversion in the expected order of $\langle N \rangle - N_P$ is observed for ^{48}Ca and ^{64}Ni at all ener-

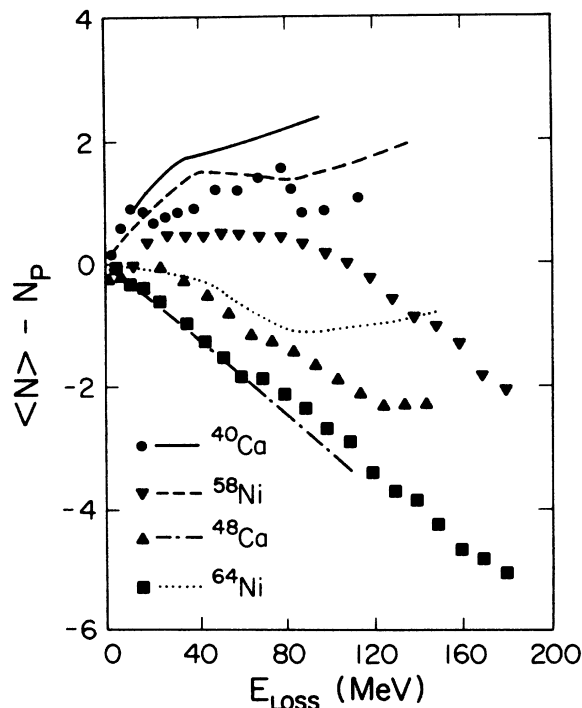


FIG. 2. Neutron drift (average measured neutron number minus the neutron number of the projectile) as a function of energy loss. See caption of Fig. 1. The systematic errors are approximately $\pm 0.4 N$ units.

gy losses. If one assumes the number of evaporated neutrons, at an $E_{\text{loss}} = 100$ MeV, to be the same for the $^{238}\text{U} + ^{40}\text{Ca}$ and $^{238}\text{U} + ^{48}\text{Ca}$ systems, the first system transfers approximately three more neutrons to the PLF than does the second system.

The behavior of the variances in the charge and neutron number distributions with respect to E_{loss} is demonstrated in Fig. 3. The variances and the correlation coefficient are needed together with the first moments to describe the evolution of the reaction product distribution in the N vs Z plane with increasing kinetic energy damping.⁷ The variances shown for the experimental data are also affected by the sequential decay of the excited primary reaction fragments.¹⁰ Although in most cases the distributions are narrowed by the evaporation process, whether evaporation narrows or broadens the initial distributions depends on the excitation energy division and the width of the primary distribution relative to the curvature of the beta stability valley.

In Randrup's dynamical reaction model^{3,4} the transport of mass, charge, and energy is mediated by the exchange of nucleons between the two partners in the dinuclear system. The corresponding transport coefficients are calculated from the instantaneous condition of the dinuclear complex, the constituents of which are always considered to be at their individual thermodynamical equilibrium. The reaction variables (q_i) include the charge Z and mass A of one of the fragments. The average values ($\bar{q}_i, \bar{\dot{q}}_i$) of the macroscopic coordinates and velocities follow the equations of motion determined by the Lagrange-

Rayleigh equations,

$$\left(\frac{d}{dt} \frac{\partial}{\partial \dot{q}_i} - \frac{\partial}{\partial q_i} \right) L = - \frac{\partial}{\partial \dot{q}_i} F, \quad (1)$$

where the subscript i runs over all reaction variables. The quantity L is the Lagrangian and F is the Rayleigh dissipation function describing the conversion of kinetic energy of relative, tangential, and neck motion into intrinsic heat energy. The driving forces affecting the evolution of the collective variables can be separated into static and dynamic components.

In this model, the fluctuations in N and Z about the average values are predicted by a Fokker-Planck equation

$$\frac{\partial}{\partial t} P(N, Z, t) = \left[- \frac{\partial}{\partial N} v_N - \frac{\partial}{\partial Z} v_Z + \frac{\partial^2}{\partial N^2} D_{NN} + \frac{\partial^2}{\partial Z^2} D_{ZZ} \right] P(N, Z, t). \quad (2)$$

describing the time dependence of the joint probability distribution $P(N, Z, t)$ for finding N neutrons, Z protons at time t in one of the reaction partners. Drift and diffusion coefficients, v and D , respectively, have been calculated microscopically by Randrup.³

The above dynamical transport calculation predicts the first and second moments of the proton (Z) and neutron (N) number distributions, as well as the excitation energies of the primary reaction fragments. To make a valid comparison with experimental data, the predicted primary distributions are subjected to a statistical evaporation calculation with the code PACE based on the fragment excitation energy division calculated within the transport model.

The results of the theoretical calculations, corrected for particle emission are shown in Figs. 1-3. The magnitude of the theoretical proton drift towards the TLF agrees well with the data for the $^{238}\text{U} + ^{48}\text{Ca}$ reaction. For the other three reactions, the observed direction of the proton drift agrees with theoretical expectations. However, its magnitude is underpredicted ($|\langle Z \rangle - Z_P|$ is too small) by approximately 1.4 Z units at an E_{loss} of 100 MeV. The direction of the neutron drift is again predicted correctly for all four reactions. In the case of the projectiles ^{40}Ca and ^{58}Ni the driving force $\Delta V/\Delta N$ is large for neutron drift to the PLF. On the other hand, for the neutron-rich projectiles, ^{48}Ca and ^{64}Ni , there is a negligible driving force, $\Delta V/\Delta N \approx 0$, and the experimental drift is dominated by neutron evaporation. At $E_{\text{loss}} = 100$ MeV, the magnitude of the deviations in $|\langle N \rangle - N_P|$ between theory and experiment is slightly larger than one neutron for all four reactions. The theory overpredicts the difference $\langle N \rangle - N_P$ for the $^{238}\text{U} + ^{48}\text{Ca}$ reaction and underpredicts this quantity for the other three reactions.

The experimental and theoretical neutron and proton variances shown in Fig. 3 are on the whole in good agreement. Hence, the theory describes the influence of restoring forces on the fluctuations from the average trajectory reasonably well. At energy losses larger than 40 MeV, the experimental values of σ_N/σ_Z are essentially constant with energy loss and somewhat smaller for the neutron-rich projectiles, ^{48}Ca and ^{64}Ni , than for the projectiles

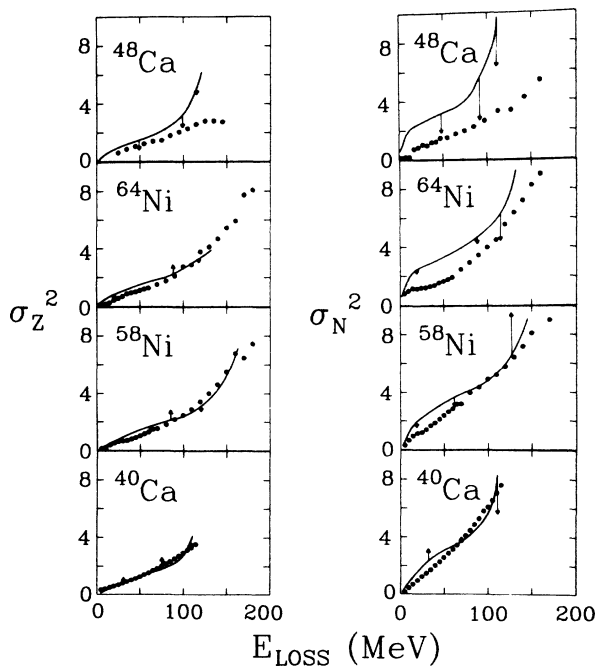


FIG. 3. The neutron variance σ_N^2 and proton variance σ_Z^2 as a function of energy loss. The solid lines represent the theory uncorrected for particle emission. See caption of Fig. 1. The arrows indicate the direction and magnitude of the correction to the theoretical variance due to the particle emission.

^{40}Ca and ^{58}Ni .

In conclusion, the first and second moments in the proton and neutron-number distributions of projectile-like fragments have been measured for four reactions where the gradients in the potential-energy surfaces vary monotonically over a wide range. The variances in the N and Z distributions are reasonably well reproduced by a dynamical reaction model; however, remaining discrepancies require improvements in the model parameters. Except for the inversion in the expected order of $\langle N \rangle - N_P$ for ^{48}Ca and ^{64}Ni , the observed trends in the neutron and proton drifts with energy loss are understood in terms of the potential-energy gradients when account is taken of particle evaporation. However, the magnitudes of the predict-

ed proton drifts are too small, indicating that the model underestimates the strength of the driving forces. These data demonstrate the need for a more quantitative theory for nucleon transport in damped reactions.

This work was supported by the U.S. Department of Energy and the National Science Foundation. The authors thank D. R. Benton, J. R. Birkelund, M. A. Butler, S. S. Datta, I. M. Govil, F. Khazaie, R. J. McDonald, A. C. Mignerey, J. Töke, A. Weston-Dawkes, W. W. Wilcke, J. L. Wile, W. G. Wilson, K. L. Wolf, H. J. Wollersheim, W. P. Zank, S. H. Zhou, and the SuperHILAC staff for their assistance.

-
- ¹W. U. Schröder and J. R. Huizenga, in *Treatise on Heavy-Ion Science*, edited by D. A. Bromley (Plenum, New York, 1984), Vol. 2, Chap. 3, and references cited therein.
²H. Freiesleben and J. V. Kratz, *Phys. Rep.* **106**, 1 (1984).
³J. Randrup, *Nucl. Phys.* **A307**, 319 (1978); **A327**, 490 (1979); **A383**, 468 (1982).
⁴W. U. Schröder, J. R. Huizenga, and J. Randrup, *Phys. Lett.* **98B**, 355 (1981).
⁵J. R. Huizenga, W. U. Schröder, J. R. Birkelund, and W. W. Wilcke, *Nucl. Phys.* **A387**, 257c (1982); T. C. Awes *et al.*, *Phys. Rev. Lett.* **52**, 251 (1984); R. Vandenbosch *et al.*, *ibid.*

- 52**, 1964 (1984); H. Sohlbach *et al.*, *Phys. Lett.* **153B**, 386 (1985); J. L. Wile, W. U. Schröder, J. R. Huizenga, and D. Hilscher, *Phys. Rev. C* **35**, 1608 (1987); D. R. Benton *et al.*, *Phys. Lett.* **185B**, 326 (1987).
⁶H. C. Britt *et al.*, *Phys. Rev. C* **26**, 1999 (1982).
⁷H. Breuer *et al.*, *Phys. Rev. C* **28**, 1080 (1983).
⁸K. Kwiatkowski *et al.*, *Nucl. Instrum. Methods* **225**, 65 (1984).
⁹A. Gavron, *Phys. Rev. C* **21**, 230 (1980).
¹⁰D. K. Lock, R. Vandenbosch, and J. Randrup, *Phys. Rev. C* **31**, 1268 (1985).